A Three-Phase Isolated Secondary-Resonant Single-Active-Bridge DC-DC Converter with a Delta-Star Connected Transformer

Atsushi Nishio, Kohei Budo, Mai Van Tuan and Takaharu Takeshita
Dept. of Electrical and Mechanical Engineering, Graduate School of Engineering,
Nagoya Institute of Technology
Gokiso, Showa
Nagoya, 466-8555 Japan
Phone: +81 (52) 735-5441
Fax: +81 (52) 735-5432
Email: take@nitech.ac.jp
URL: http://motion.web.nitech.ac.jp/

Acknowledgments

A part of this work was supported by JSPS KAKENHI Grant Number JP21H01310.

Keywords

≪Power converters for EV≫, ≪Converter circuit≫, ≪DC-DC converters≫, ≪Soft switching≫, ≪Three-phase system≫

Abstract

This paper presents a three-phase isolated secondary-resonant single-active-bridge DC-DC converter with a delta-star connected transformer. The total power factor of the transformer can be improved by using the LC resonance compared with a conventional converter. The effectiveness of the proposed circuit is verified by experiments using a 2.5 kW 265 V, 15 kHz laboratory prototype.

Introduction

Lately, various problems such as global warming and the energy crisis have happened. The spread of electric vehicles (EVs) is one of the solutions to solve these problems. Recently, many kinds of isolated DC-DC converters have been researched and developed for applications of battery chargers [1]-[8]. There are two types of isolated DC-DC converters: single-phase circuits and three-phase circuits. A three-phase isolated DC-DC converters are suitable for a high-power conversion compared with a single-phase one [9]. By these reasons, the demand for a three-phase isolated DC-DC converter increases.

Various topologies of three-phase isolated DC-DC converters has been proposed. The single-active-bridge (SAB) DC-DC converter [5],[9],[10] for an unidirectional power converter has been proposed. It has a three-phase inverter on the primary side and a diode rectifier circuit on the secondary side. Because the secondary side of the transformer is composed of a diode rectifier circuit, there are few numbers of necessary parts, and this circuit can be downsized. Furthermore, it can reduce a switching loss by using soft-switching. A three-phase isolated DC-DC converter has four types of transformer connections, star-star connection, delta-delta connection, delta-star connection, and star-delta connection. The SAB can achieve high-efficiency and high power density by using star-delta or delta-star connection of the transformer [11]. Because the secondary circuit of the SAB is composed of diodes, the value of the total power factor of the transformer becomes low. Therefore, a loss becomes large.

This paper presents a three-phase isolated secondary-resonant single-active-bridge (SR-SAB) DC-DC converter. The proposed circuit is more suitable for high power applications than single-phase SR-SAB

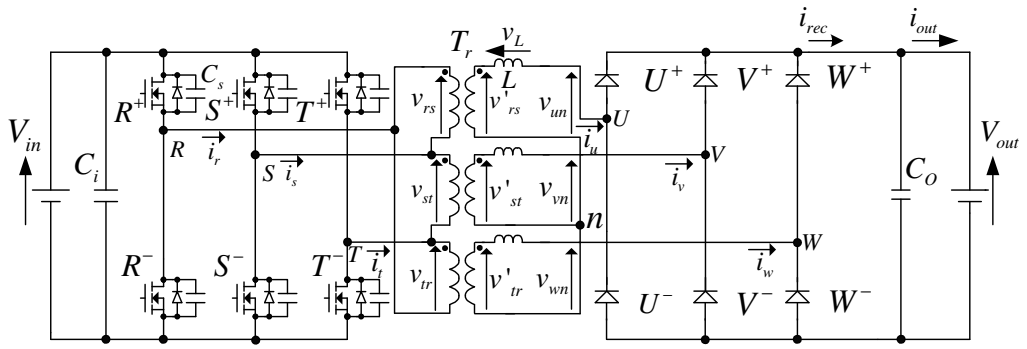

(a) Conventional three-phase isolated SAB DC-DC converter with a delta-star connected transformer.

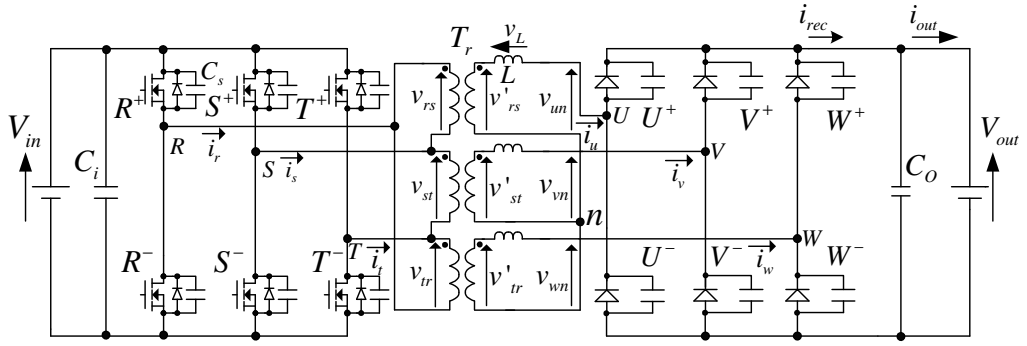

(b) Proposed three-phase isolated SR-SAB DC-DC converter with a delta-star connected transformer.

Fig. 1: Isolated three-phase DC-DC converter.

[3],[4] because it uses a three-phase transformer. The primary side of the transformer is composed of a three-phase inverter, the secondary side of the transformer consists of a diode rectifier circuit composed of six diodes with the resonant capacitor in parallel. The SR-SAB can achieve soft-switching. The SR-SAB can also raise the value of the total power factor of the transformer because the SR-SAB can smoothly change a transformer current by using the LC resonance between the leakage inductor of the transformer and the resonant capacitor. The theory of a three-phase isolated SR-SAB DC-DC converter with a delta-star connected transformer is derived, and the effectiveness of the theory is verified by experiments.

Overview of Three-Phase Isolated DC-DC Converter

Circuit Configuration of a Conventional SAB Converter

Fig. 1(a) shows a conventional three-phase isolated SAB DC-DC converter with a delta-star connected transformer. The SAB is an isolated DC-DC converter. The primary circuit of the high frequency transformer T_r is composed of a three-phase inverter composed of six switches $R^+ - T^-$ with the soft-switching capacitors C_s in parallel. The secondary circuit is composed of a three-phase diode rectifier circuit composed of six diodes $U^+ - W^-$. When the input DC voltage V_{in} and the output DC voltage V_{out} are equal, transformer current i_u does not flow. Therefore, the SAB cannot send electric power to the load V_{out}. The SAB needs the higher input voltage V_{in} than the output voltage V_{out}, and then the value of the total power factor of the transformer becomes low.

Circuit Configuration of a Proposed SR-SAB Converter

Fig. 1(b) shows a proposed three-phase isolated SR-SAB DC-DC converter with a delta-star connected transformer. The primary circuit of the high frequency transformer T_r is the same configuration as the SAB in Fig. 1(a). The difference from the conventional circuit is the configuration of the secondary circuit. The secondary circuit is composed of a three-phase diode rectifier circuit composed of six diodes

$U^+ - W^-$ with the resonant capacitor C_r in parallel. To make V_{in} and V_{out} equal, the turn ratio of the transformer is set to 2:1. The proposed circuit can reduce switching loss by achieving soft-switching in the primary side. The proposed circuit can reduce a recovery loss on the diode because the recovery current does not flow in the secondary diode-bridge by the LC resonance. Since LC resonance occurs at the leakage inductance L of the high-frequency transformer T_r and the capacitor C_r, electric power can be sent even in situations when input and output voltages are equal. The total power factor of the transformer is also improved.

Advantages of a Proposed SR-SAB

Fig. 2 shows the switching patterns of the primary phases R, S and T and the voltage and current waveforms of the high frequency transformer. The waveforms were generated under the same output power, 3.0 kW. The simulation conditions of the waveforms are shown in Table I. The blue line shows waveforms of a conventional SAB converter, the red line shows waveforms of a proposed SR-SAB converter. The square voltage waveform v'_{rs} with voltage level 0, $\pm V_{in}/2$ is generated by using the switches of phases R and S are switched every 120 degrees and their duty ratios are 50 %. The primary voltage $v'_{rs}(= v_{rs}/2)$ is the secondary equivalent voltage of the primary voltage taking into account that the transformer turn ratio is 2:1. The secondary voltage v_{un} is the line voltage on the secondary side of the transformer. The voltage v_L is the voltage difference between the primary voltage v'_{rs} and the secondary voltage v_{un}, and the transformer current i_u flows when this voltage is applied to the transformer. The durations T_0 shown in Fig. 2 is the period when LC resonance is occurred in the phase R.

The waveforms of the SAB are shown in Fig. 2 as blue lines. The output DC voltage V_{out} is 265 V, and the input DC voltage V_{in} is raised to 360 V to obtain the output power P_{out}, 3.0 kW. The primary voltage v'_{rs} is square voltage waveform with voltage level 0, $\pm V_{in}/2$. The secondary voltage v_{un} is square voltage waveform with voltage level 0, $\pm V_{out}/3$, $\pm 2V_{out}/3$. The transformer current i_u becomes trapezoidal waveform.

The waveforms of the SR-SAB under the condition $V_{in} = V_{out}$ are shown in Fig. 2 with red lines. The primary voltage v'_{rs} is the square voltage waveform with voltage level 0, $\pm V_{in}/2$. During the period of T_0 shown in the Fig. 2, LC resonance is occurred and the secondary voltage v_{un} varies sinusoidally. In the period T_0, the reactor voltage v_L becomes large because the voltage difference between the primary and secondary voltages increases, and the transformer current i_u increases sinusoidally. The transformer current i_u of the SR-SAB becomes a near sinusoidal waveform.

The SR-SAB can make a phase difference be-

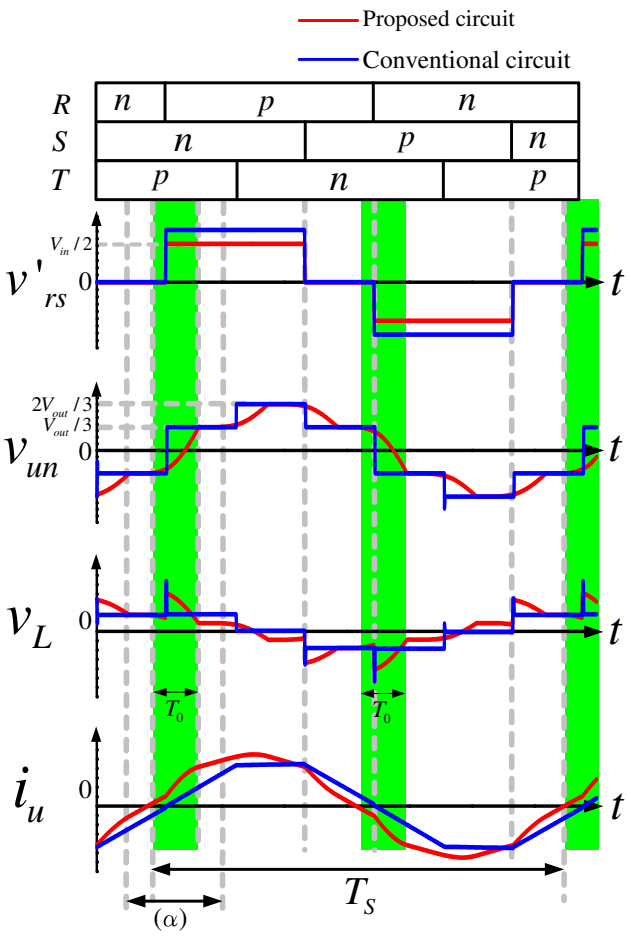

Fig. 2: Theoretical waveforms.

Table I: Simulation conditions.

Parameter	SAB	SR-SAB
Output power P_{out}	3.0 kW	
Output voltage V_{out}	265 V	
Input voltage V_{in}	360 V	265 V
DC capacitors C_i, C_o	1500 μF	
Resonant capacitor C_r	–	80 nF
Leakage inductance L	93 μH	
Frequency of transformer f_s	15 kHz	
Total Power Factor	0.78	0.92

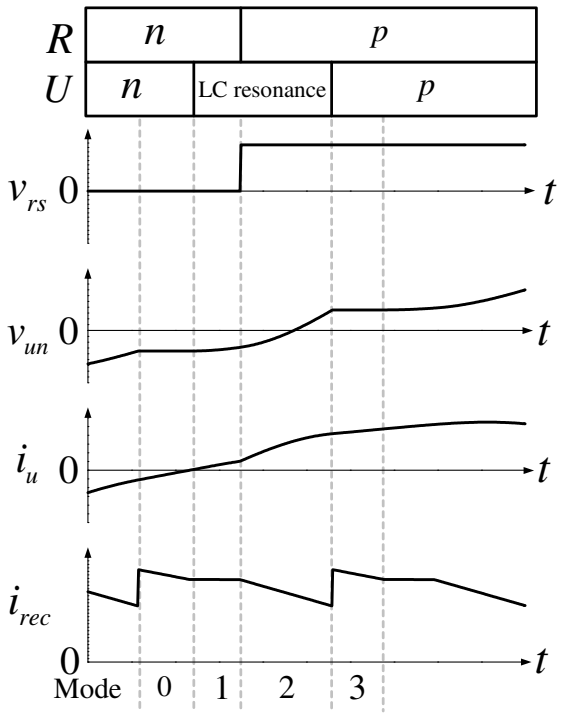

Fig. 3: Magnification waveforms of proposed circuit.

tween the primary voltage v'_{rs} and the secondary voltage v_{un} by using LC resonance. The waveform value of the reactor voltage v_L of the SR-SAB is higher than that of the SAB, especially during the LC resonance term. The transformer current i_u is increased significantly during the LC resonance term when the phase difference between the primary voltage v'_{rs} and the secondary voltage v_{un} becomes particularly large.

The total power factor of the transformer is obtained as (1) by using the value of the output power P_{out}, the effective value of the primary voltage V_{rsrms} and the effective value of the primary transformer current I_{rrms}. The total power factor under the simulation conditions is calculated to be 0.78 for the SAB and 0.92 for the SR-SAB. This is why the SR-SAB is better suited for high power conversion than the SAB.

$$TPF = \frac{P_{out}}{3 \times V_{rsrms} \times I_{rrms}} \tag{1}$$

Switching Operation of the Proposed Circuit

The magnified waveforms of the theoretical waveforms in Fig. 2 are shown in Fig. 3. The period of (α) is divided into four operation modes Mode 0−Mode 3. The switching pattern of the primary phase R and the conduction pattern of the secondary phase U are also shown. The current i_{rec} is generated by being rectified the transformer current i_u, i_v and i_w. The switches of phase R are switched when shifting from Mode 1 to Mode 2. The diode of the phase U turns off when the operation mode changes from Mode 0 to Mode 1, then LC resonance occurs in Modes 1 and 2, and conduction resumes when Mode 3 begins. Thus, the switching timing of the switch on the primary side and the conduction timing of the diode on the secondary side are offset by caused LC resonance in the secondary side circuit. The voltage difference between the primary voltage v_{rs} and the secondary voltage v_{un} becomes larger in Mode 1 and Mode 2 by the secondary voltage v_{un} increased gradually by LC resonance, to avoid switching timing of the diode on the secondary side at the same timing as the switching of the switch on the primary side. In this way, the transformer current i_u is increased significantly. This is the reason that power can be converted even when the input DC voltage V_{in} and output DC voltage V_{out} are equal or when the input DC voltage V_{in} is lower. These characteristics indicate that the proposed the SR-SAB is more suitable for high power conversion than conventional the SAB.

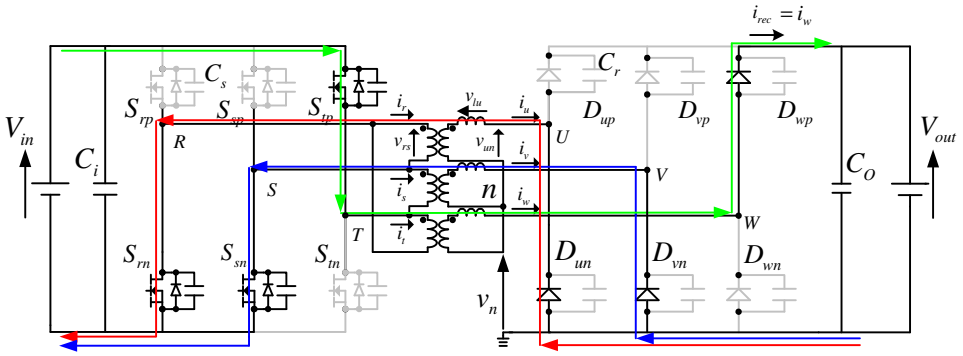

(a) Mode 0

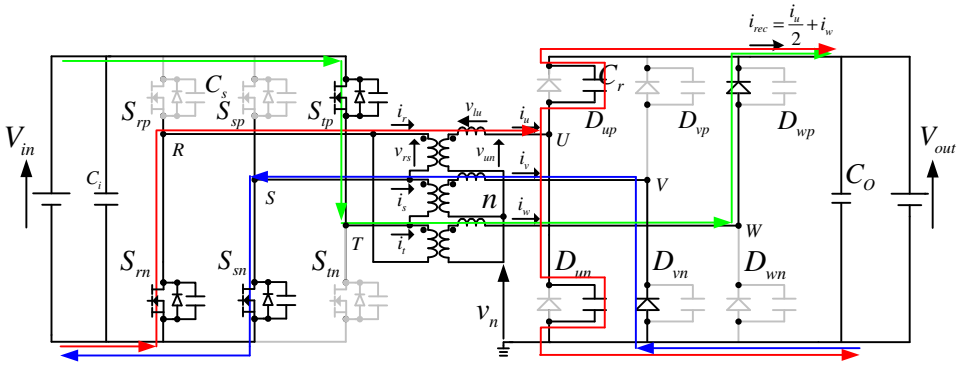

(b) Mode 1

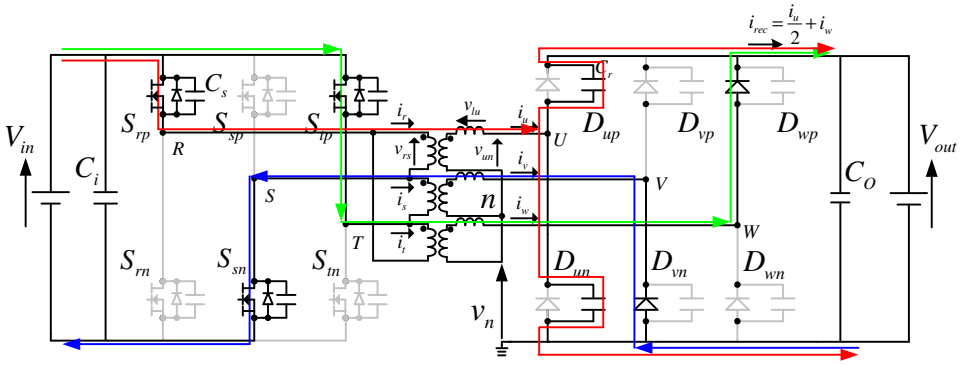

(c) Mode 2

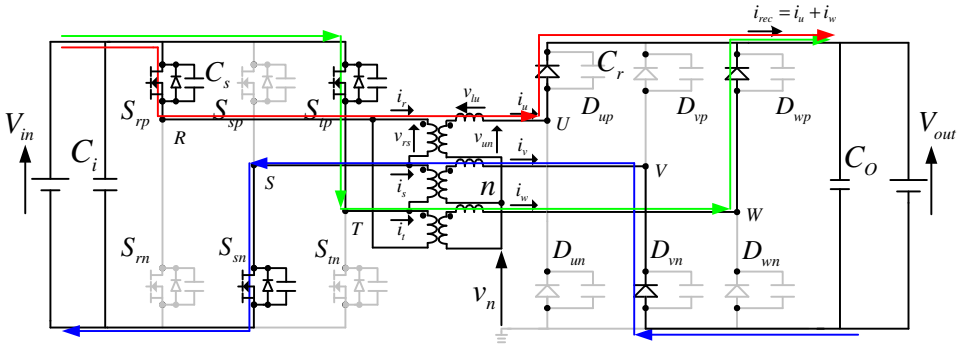

(d) Mode 3

Fig. 4: Connection diagram of the proposed SR-SAB.

Theory of Secondary Converter

Fig. 4 shows the commutation modes from the diode U^- to U^+ on the secondary diode rectifier circuit. In Mode 0, the diode U^- is conducting, and after the resonance period of Mode 1 and Mode 2, the diode U^+ is conducting in Mode 3. Fig. 3 shows the magnification of the theoretical waveforms in Fig. 2. The diode U^- becomes on-state during Mode 0, and diodes U^- and U^+ become off-state during Mode 1, and the diode U^+ becomes on-state during Mode 3. In Mode 0, the primary voltage v'_{rs} is zero. As the diode U^- is on-state, the secondary voltage v_{un} is $-V_{out}/3$, and the transformer current i_u increases by the difference of the primary voltage v'_{rs} and the secondary voltage v_{un}. When the transformer current i_u becomes zero, the circuit becomes to Mode 1. In Mode 1, the diode U^- becomes off-state, and the LC resonance between the leakage inductor L and two capacitors C_r connected parallel to diodes U^+ and U^- occurs. The transformer current i_u increases from zero, and the secondary voltage v_{un} is the sinusoidal waveform in Mode 1. When the on-state switch of three-phase inverter of the primary side is switched from R^- to R^+ during Mode 1, the primary voltage v'_{rs} becomes $V_{out}/2$. Mode 1 is finished then. In Mode 2, the transformer current i_u continues increasing, and the secondary voltage v_{un} also increases in the sinusoidal waveform by the LC resonance like Mode 1. When the secondary voltage v_{un} becomes $V_{out}/3$, the diode U^+ becomes on-state, the circuit becomes to Mode 3. In Mode 3, the primary voltage v'_{rs} is $V_{out}/2$ and the secondary voltage v_{un} is $V_{out}/3$, and therefore the transformer current i_u increases. The following voltage equation of the transformer in Fig. 4 is obtained:

$$\begin{bmatrix} v'_{rs} \\ v'_{st} \\ v'_{tr} \end{bmatrix} = \frac{L}{3}\frac{d}{dt}\begin{bmatrix} i_u \\ i_v \\ i_w \end{bmatrix} + \begin{bmatrix} v_u \\ v_v \\ v_w \end{bmatrix} - \begin{bmatrix} v_n \\ v_n \\ v_n \end{bmatrix} \tag{2}$$

The voltage v_n is obtained in (3) by using the relations $i_u + i_v + i_w = 0$ and $v'_{rs} + v'_{st} + v'_{tr} = 0$ in (2):

$$v_n = \frac{1}{3}(v_u + v_v + v_w) \tag{3}$$

Mode 1

Fig. 4(b) shows the connection diagram of Mode 1. Under the condition that the time when the transformer current i_u becomes zero is defined as $t = 0$, and the time when the primary-side of the circuit switches during LC resonance is determined as T_1, the period from $t = 0 - T_1$ is Mode 1. When the transformer current i_u becomes zero, the diodes U^+ and U^- are turned off, and the current flows to the reactor L and the capacitors C_r equally. Therefore, the capacitor of the diode U^+ is discharged and the capacitor of the diode U^- is charged by half of the transformer current i_u. The voltage waveform and the current waveform becomes sinusoidal waveform by LC resonance. The voltage of the phase U v_u is obtained as follows:

$$v_u = \frac{1}{2C_r}\int i_u dt \tag{4}$$

The neutral point potential v_n is calculated in (5):

$$v_n = \frac{1}{3}V_{out} + \frac{1}{6C_r}\int i_u dt \tag{5}$$

The secondary interline voltage of the transformer in Fig. 4(b) is obtained from (4) and (5):

$$v_{un} = v_u - v_n = -\frac{1}{3}V_{out} + \frac{1}{6C_r}\int i_u dt \tag{6}$$

The voltage equation of the phase U of Mode 1 is obtained as follows:

$$\frac{1}{3}V_{out} = \frac{1}{3}L\frac{di_u}{dt} + \frac{1}{3C_r}\int i_u dt \tag{7}$$

The transformer current i_u in Fig. 4(b) is calculated from (7):

$$i_u(t) = V_{out}\sqrt{\frac{C_r}{L}}\sin\frac{t}{\sqrt{LC_r}} \tag{8}$$

The resonant frequency f_0 is obtained:

$$f_0 = \frac{1}{2\pi\sqrt{LC_r}} \tag{9}$$

The transformer current in the phase where the LC resonance occurs becomes a sinusoidal waveform with the resonant frequency f_0. Substituting the transformer current i_u in (8) into (4), the voltage v_u is calculated as follows:

$$v_u(t) = \frac{1}{2}V_{out}\left(1 - \cos\frac{t}{\sqrt{LC_r}}\right) \tag{10}$$

The secondary interline voltage of the transformer v_{un} in Fig. 4(b) is obtained from (7):

$$v_{un} = v_u - v_n = -\frac{1}{3}V_{out}\cos\frac{t}{\sqrt{LC_r}} \tag{11}$$

The secondary interline voltage of the transformer v_{un} becomes sinusoidal waveform during LC resonance. Since $v_v = 0$ and $v_w = V_{out}$ in Mode 1, and at $t = 0$, $i_u = 0$, $i_v = -I_0$ and $i_w = I_0$, so the transformer currents i_v and i_w in Fig. 4(b) are obtained by (2):

$$i_v(t) = -I_0 - \frac{1}{2}i_u(t) \tag{12}$$

$$i_w(t) = I_0 - \frac{1}{2}i_u(t) \tag{13}$$

While the transformer current i_u increases, both transformer currents i_v and i_w decrease. The output current i_{rec} in Fig. 4(b) is obtained as follows:

$$i_{rec}(t) = \frac{1}{2}i_u(t) + i_w(t) = I_0 \tag{14}$$

From (14), the output current i_{rec} becomes a constant value.

Mode 2

Fig. 4(c) shows the connection diagram of Mode 1. Mode 2 continues from the time the primary circuit switches during the LC resonance of Mode 1 to the time the diode U^+ conducts. The voltage and current waveform becomes sinusoidal by the LC resonant as the same as Mode 1. The transformer current i_u increases more significantly because the resonant current in Mode 2 is added to the resonance current in Mode 1. When the value of v_u equals to V_{out}, Mode 2 is finished. The voltage equation of

phase U in Mode 2 is obtained as follows:

$$\frac{1}{6}V_{out} = \frac{L}{3}\frac{di_u}{dt} + \frac{1}{3C_r}\int i_u dt \tag{15}$$

The transformer current i_u in Fig. 4(c) is calculated by (15) as follows:

$$i_u(t) = i_{u1}(t) + i_{u2}(t) \tag{16}$$

$$i_{u1}(t) = V_{out}\sqrt{\frac{C_r}{L}}\sin\frac{t}{\sqrt{LC_r}} \tag{17}$$

$$i_{u2}(t) = \frac{3}{2}V_{out}\sqrt{\frac{C_r}{L}}\sin\frac{t-T_1}{\sqrt{LC_r}} \tag{18}$$

The first term $i_{u1}(t)$ on the right-hand side of (17) is the resonant current flows in Mode 1, and the second term $i_{u2}(t)$ is the resonant current which is appeared in Mode 2. The frequency of the resonant current $i_{u2}(t)$ is f_0. Since the resonant current $i_{u2}(t)$ is 1.5 times larger in amplitude than $i_{u1}(t)$, the resonant current $i_u(t)$ increases significantly in Mode 2 compared to Mode 1. The voltage v_u of the midpoint voltage of phase U and the interline voltage of the secondary side v_{un} in Fig. 4(c) are obtained by the following equations:

$$v_u = v_u(T_1) + \frac{1}{2C_r}\int i_u dt = V_{out}\left(\frac{5}{4} - \frac{1}{2}\cos\frac{t}{\sqrt{LC_r}} - \frac{3}{4}\cos\frac{t-T_1}{\sqrt{LC_r}}\right) \tag{19}$$

$$v_{un} = v_u - v_n = -\frac{1}{3}V_{out}\cos\frac{t}{\sqrt{LC_r}} + \frac{1}{2}V_{out}\left(1 - \cos\frac{t-T_1}{\sqrt{LC_r}}\right) \tag{20}$$

The voltage v_u and v_{un} increase more significantly than Mode 1. When the phase U voltage v_u satisfies the rerlation $v_u = V_{out}$, the diode U^+ conducts and Mode 2 finishes. The following equation is obtained from the relation of $v_u(T_1+T_2) = V_{out}$, the duration of Mode 2 is T_2 :

$$2\cos\frac{T_1+T_2}{\sqrt{LC_r}} + 3\cos\frac{T_2}{\sqrt{LC_r}} = 1 \tag{21}$$

The transformer current i_v and i_w in Fig. 4(c) is obtained from the (2) as follows:

$$i_v(t) = -I_0 + \frac{3V_{out}}{4L}(t-T_1) - \frac{1}{2}i_u(t) \tag{22}$$

$$i_w(t) = I_0 - \frac{3V_{out}}{4L}(t-T_1) - \frac{1}{2}i_u(t) \tag{23}$$

The transformer current i_v and i_w vary with the half amplitude of the resonant current i_u. The output current i_{rec} in Fig. 4(c) is obtained:

$$i_{rec}(t) = \frac{i_u}{2} + i_w = I_0 - \frac{3V_{out}}{4L}(t-T_1) \tag{24}$$

The output current i_{rec} in Mode 2 decreases at a constant rate with a slope $3V_{out}/4L$.

Mode 3

Fig. 4(d) shows the connection diagram of Mode 1. In Mode 3, the transformer currents are i_u>0, i_v<0, i_w>0, so diodes U^+, V^-, W^+ are on state. The voltage v_u between the diodes U^+ and U^- becomes $v_u = V_{out}$. In the same way, the voltages v_v and v_w are $v_v = 0$ and $v_w = V_{out}$. From (4), the neutral point potential v_n is obtained as $v_n = 2V_{out}/3$. From the voltage equation (2), the transformer currents $i_u - i_w$

are obtained as follows by using the initial current values $i_u(T_1+T_2)$, $i_v(T_1+T_2)$, $i_w(T_1+T_2)$:

$$\begin{cases} i_u(t) = i_u(T_1+T_2) + \dfrac{V_{out}}{2L}(t-T_1-T_2) \\ i_v(t) = i_v(T_1+T_2) + \dfrac{V_{out}}{2L}(t-T_1-T_2) \\ i_w(t) = i_w(T_1+T_2) - \dfrac{V_{out}}{L}(t-T_1-T_2) \end{cases} \tag{25}$$

From (25), the transformer currents i_u and i_v in Fig. 4(d) increase at a constant slope $V_{out}/2L$ and the transformer current i_w decreases at a constant slope V_{out}/L. Mode 3 is finished when the transformer current i_w becomes zero. The following relation stands for the initial current of Mode 1 I_0:

$$I_0 = i_u(T_1+T_2+T_3) = -i_v(T_1+T_2+T_3) \tag{26}$$

The initial current value of Mode 1 I_0 is obtained as follows:

$$I_0 = \frac{3V_{out}}{2L}(T_2+T_3) \tag{27}$$

Using the equations $T_1+T_2+T_3 = T_s/6$ and $T_s = 1/f_s$, the initial value I_0 is obtained as follows:

$$I_0 = \frac{3V_{out}}{2L}\left(\frac{1}{6f_s} - T_1\right) \tag{28}$$

The output current i_{rec} in Fig. 4(c) is calculated by $i_{rec} = i_u + i_w$ as follows:

$$\begin{aligned} i_{rec} &= i_u(T_1+T_2) + i_w(T_1+T_2) - \frac{V_{out}}{2L}(t-T_1-T_2) \\ &= \frac{3V_{out}}{2L}(T_2+T_3) - \frac{3V_{out}}{4L}T_2 + \frac{1}{2}V_{out}\sqrt{\frac{C_r}{L}}\sin\frac{T_1+T_2}{\sqrt{LC_r}} \\ &+ \frac{3}{4}V_{out}\sqrt{\frac{C_r}{L}}\sin\frac{T_2}{\sqrt{LC_r}} - \frac{V_{out}}{2L}(t-T_1-T_2) \end{aligned} \tag{29}$$

In Mode 3, the output current i_{rec} in Mode 3 decreases with a constant slope $V_{out}/2L$.

Experimental Results

Table II shows the experimental conditions. Fig. 5 shows the experimental waveforms under the condition of Table II. The waveforms of the primary voltage v_{rs} and the secondary voltage v_{un} are shown in Fig. 5. The waveform of the transformer current i_u is shown in Fig. 5.

The theoretical waveforms are obtained by experiments. The input power P_{in} and the output power P_{out} are measured by power analyzer WT1600, YOKOGAWA. The input power is 2.6 kW and the output power is 2.5 kW. The measured efficiency of the circuit is 95.3 %.

Table II: Experimental conditions.

Parameter	Value
Output power P_{out}	2.5 kW
Input voltage V_{in}, Output voltage V_{out}	265 V
DC capacitors C_i, C_o	1500 μF
Resonant capacitor C_r	80 nF
Leakage inductance L	93 μH
Turn ratio of the transformer	2:1
Frequency of transformer f_s	15 kHz

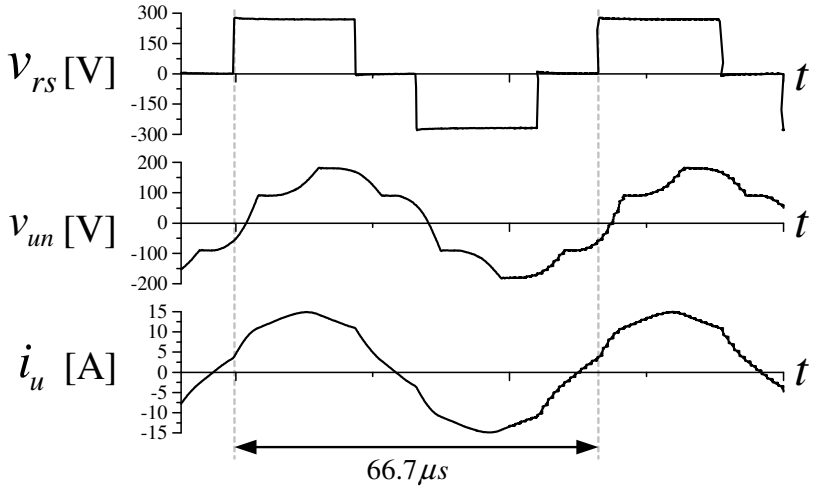

Fig. 5: Experimental waveforms. ($V_{in} = V_{out} = 265$ V, $f_s = 15$ kHz)

Conclusions

This paper presents the three-phase isolated SR-SAB DC-DC converter with a delta-star connected transformer. The advantages of the SR-SAB are clarified by comparing with the conventional SAB. The proposed SR-SAB converter can achieve high-efficiency compared with the conventional SAB by improving the value of the total power factor, and reducing the recovery loss of the diodes by the LC resonance between the leakage inductor and the capacitor of the diode rectifier circuit. The effectiveness of the theory is verified by experiments.

References

[1] R. W. A. A. De Doncker, D. M. Divan and M. H. Kheraluwala, "A three-phase soft-switched high-power-density DC/DC converter for high-power applications," *in IEEE Transactions on Industry Applications,* vol. 27, no. 1, pp. 63-73, Jan.-Feb. 1991

[2] C. Meyer and R. W. De Doncker, "Design of a Three-Phase Series Resonant Converter for Offshore DC Grids," *2007 IEEE Industry Applications Annual Meeting,* 2007, pp. 216-223

[3] Tuan, C.A.; Takeshita,T. "Analysis of Unidirectional Secondary Resonant Single Active Bridge DC-DC Converter," *Energies 2021,* 14, 6349, 2022, p.14

[4] Cao Anh Tuan, Takaharu Takeshita, "Output Power Characteristics of Unidirectional Secondary-Resonant Single-Active-Bridge DC-DC Converter using Pulse Width Control," *IEEJ Journal of Industry Applications,* Volume 11, Issue 2, 2022, pp. 359-368

[5] Y. Sang, A. Junyent-Ferré and T. C. Green, "Operational Principles of Three-Phase Single Active Bridge DC/DC Converters Under Duty Cycle Control," *in IEEE Transactions on Power Electronics,* vol. 35, no. 8, pp. 8737-8750, Aug. 2020

[6] Yeh Ting, S. de Haan and J. A. Ferreira, "A DC-DC Full-Bridge Hybrid Series Resonant Converter enabling constant switching frequency across wide load range," *Proceedings of The 7th International Power Electronics and Motion Control Conference,* 2012, pp. 1143-1150

[7] M. Stieneker and R. W. De Doncker, "Dual-active bridge dc-dc converter systems for medium-voltage DC distribution grids," *2015 IEEE 13th Brazilian Power Electronics Conference and 1st Southern Power Electronics Conference (COBEP/SPEC),* 2015, pp. 1-6

[8] J. Jacobs, A. Averberg and R. De Doncker, "Multi-Phase Series Resonant DC-to-DC Converters: Stationary Investigations," *2005 IEEE 36th Power Electronics Specialists Conference,* 2005

[9] C. Sommer, A. Mertens, I. Larrazabal and I. Kortazar, "Analytical investigation of the three-phase single active bridge for offshore applications," *2016 18th European Conference on Power Electronics and Applications (EPE'16 ECCE Europe),* 2016, pp. 1-10

[10] Y. Ting, S. de Haan and J. A. Ferreira, "The partial-resonant single active bridge DC-DC converter for conduction losses reduction in the single active bridge," *2013 IEEE ECCE Asia Downunder,* 2013, pp. 987-993

[11] J. Jacobs, M. Thommes and R. De Doncker, "A transformer comparison for three-phase single active bridges," *2005 European Conference on Power Electronics and Applications,* 2005, pp. 10 pp.-P.10